ChemComm
Chemical Communications

Accepted Manuscript

This article can be cited before page numbers have been issued, to do this please use: G. Jobin and M. W. Drover, *Chem. Commun.*, 2026, DOI: 10.1039/D6CC01343K.

ROYAL SOCIETY OF CHEMISTRY

rsc.li/chemcomm

View Article Online
DOI: 10.1039/D6CC01343K

COMMUNICATION

A Dual-Metal Strategy for *N*-Heterocycle Coordination Using Nickel and Aluminum

Received 00th February 2026
Accepted 00th February 2026

DOI: 10.1039/x0xx00000x

Gabriel J. Jobin[a] and Marcus W. Drover[a,*]

Heterobimetallic Lewis acid/transition-metal systems aid heterocycle upgrading, yet well-defined cooperative examples remain scarce. We present a new ambiphilic phosphorus/aluminium ligand that preorganizes pyridine and quinoline for nickel coordination, affording well-defined co-activated η² heterocycle complexes that represent commonly proposed, but rarely observed, intermediates in *N*-heterocycle upgrading.

Nitrogen-containing heterocycles are ubiquitous in biologically active molecules, comprising approximately 82% of FDA-approved drugs from 2013-23.[1,2] The selective functionalization of these privileged motifs remains a central objective in synthetic chemistry, particularly due to the difficulty of achieving site-selective C–H bond activation.[3,4] Transition metal-catalyzed C–H bond activation offers a promising avenue, yet the inherent Lewis basicity of *N*-heterocycles often leads to unproductive or poorly selective outcomes.[5]

A detailed understanding of substrate coordination behavior is critical for expanding the toolkit of heterocycle functionalization strategies. Key mechanistic questions: how is substrate activated? what is the role of the ligand? how do geometric constraints govern product formation? lie at the heart of ligand and catalyst design. One emerging strategy involves heterobimetallic complexes, in which a main-group Lewis acid cooperatively engages a substrate alongside a transition metal catalyst.[1,6–24] In such systems, the Lewis acid (e.g., a trivalent aluminum species) serves to anchor the *N*-heterocycle in a defined orientation, thereby facilitating selective coordination by an adjacent transition metal.[9,10,25]

Progress in this area has been marked by the use of trivalent aluminum additives as components of "catalytic cocktails" where Al and a transition metal (often nickel) work in synergy to co-activate a given substrate (**Scheme 1a**).[15,26,27] While mixtures of Al, Ni, and L-type donor ligands such as carbenes and phosphines have been proven adept for *N*-heterocycle upgrading catalysis, examples where substrate has been unambiguously characterized in the coordination spheres of both metals are rare.[13] A notable exception is the 2010 work of Yap and co-workers, who reported the crystallographic characterization of a Ni(0)-Al(III) η^2-pyridine intermediate, displaying a formal N—Al dative interaction with Ni(0) coordinating to the pyridine π-system, (**Scheme 1b**). This dual activation prevents the more common coordination mode associated with pyridine(*N*) acting as a σ-donor to Ni, and was shown to be catalytically relevant, serving as an intermediate in the selective *para*-alkynylation of heteroaryl substrates (**Scheme 1b**).[13]

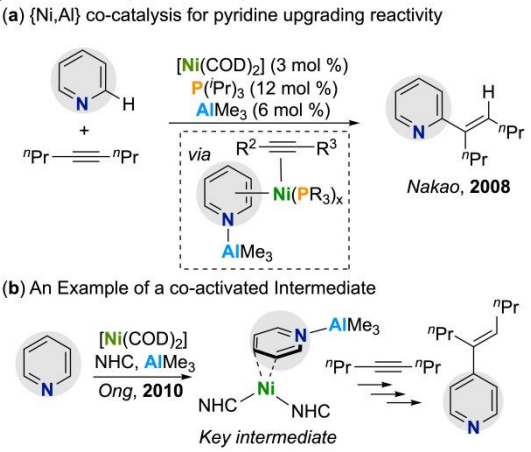

Scheme 1. (**a**) {Ni,Al} Co-catalysis for Pyridine Upgrading Reactivity; (b) An Example of a Co-activated Intermediate.

While ill-defined mixtures of {Al, Ni, and L-type ligands} have seen application in *N*-heterocycle functionalization, bringing all three components (Ni(L_n), Al, substrate) together comes at a significant entropic cost, often requiring high concentrations of aluminum additive. Ambiphilic ligands comprising a donor (such as a phosphine) and pendent Lewis acid reduce the barrier for substrate activation.[6,28] For {Ni,Al} heterometallics, so-called ambiphilic ligands have shown improved selectivity and reactivity, due to synergistic directing effects.[9,29] Implementation of such scaffolds has enabled catalytic transformations not readily accessible using traditional ligand architectures, including unconventional C3-selective pyridine olefination.[7]

Here, we report the isolation and characterization of a novel aluminum–phosphorus ambiphilic ligand that enables cooperative η²-pyridine/quinoline coordination. This distinctive binding motif arises from a cooperative interaction between a secondary-sphere aluminum(III) Lewis acid and a nickel(0) center. The emergence of this motif provides key structural insight into the nature of substrate activation within a bimetallic system.[30,31] Using this pair, dual activation of the heterocycle is achieved using a nickel–diphosphine template[32] featuring a secondary coordination sphere Lewis acid.

[a] *Department of Chemistry, Western University, 1151 Richmond St, London, ON, N8K 3G6, Canada * E-mail: marcus.drover@uwo.ca*
Supplementary Information available: Experimental details, spectroscopic data, and computational methods. See DOI: 10.1039/x0xx00000x

The phosphine electrophile, **1** was selected as a suitable host for introduction of both phosphine and alane functionality. The polarized P—I bound in **1** readily reacts with *o*-bromobenzylmagnesium at -78 °C to afford **2**, bearing three bulky *tert*-butyl groups and an *ortho*-benzyl bromide site amenable to Lewis acid introduction (**Scheme 1**).[33] Perfluoroaryl rings significantly enhance Lewis acidity, and so $\{Cl\text{-}Al(C_6F_5)_2\}_2$ was selected as the alane partner of choice. To facilitate lithium halogen exchange, **2** was reacted with 1 equiv. of *n*-BuLi and stirred at room temperature. Addition of 0.5 equiv. $\{Cl\text{-}Al(C_6F_5)_2\}_2$ quenched reaction color and after filtration, **3** was isolated as a colorless oil in 81% yield. It is important to note that despite repeated purification attempts, including variation of solvent systems and crystallization conditions, compound **3** could not be isolated in 100% analytically pure form and contained some -P(^{t}Bu)$_2$-contianing impurities (**Figure S3**), however, it remains a valuable precursor to coordination complexes (*vide infra*), whose distinct solubility profiles enabled more straightforward purification. By atmospheric pressure chemical ionization mass spectrometry (APCI-MS), a $[M]^+$ signal at *m/z* = 713.211 (calcd. = 713.210 for $C_{33}H_{38}AlF_{10}P_2$) of the appropriate isotope pattern was observed. By $^{31}P\{^1H\}$ NMR spectroscopy, two doublets in a 1:1 ratio at δ_P = 37.4 and 1.13 ppm ($J_{P,P}$ = 39.3 Hz) were additionally seen for **3**; notably, the upfield shifted signal is significantly broadened due to the presence of an intramolecular P—Al interaction (owing to the quadrupolar nature of ^{27}Al nucleus (*I* = 5/2)). $^{19}F\{^1H\}$ NMR spectroscopy further supported adduct formation, with the distance between *para*- and *meta*-aryl fluorine signals being close ($\Delta_{p,m}$ = 8.2 ppm).[34] Formation of a five membered -P-(C)$_3$-Al ring is additionally shown by significant splitting of the benzylic CH_2 protons, which appear as two doublets of doublets at δ_H = 3.21 and 2.63 ppm ($^2J_{H,H}$ = 16.4 Hz). These peaks are significantly shifted from precursor **2**, which has overlapping benzylic signals at δ_H = 2.93 ppm.[33]

The Lewis acid-base interaction in **3** is highly stabilizing. Computational analysis of the ring-opened and -closed forms reveals an energy difference of ΔG° = -22.6 kcal mol^{-1} in favor of the ring-closed product. Taking advantage of the ability of aluminum to host coordination numbers greater than four, we wondered if the ring system in **3** could be 'primed' for metal-induced ring-opening through addition of a target *N*-heterocycle, granting a five-coordinate aluminum adduct.

In a representative reaction, complex **3** was reacted with pyridine. Upon treatment of **3** with 1.5 equivs. pyridine, two new signals at δ_P = 37.3 and -1.10 ppm were observed by $^{31}P\{^1H\}$ NMR spectroscopy; for the signal ascribed to the P-(C)$_3$-Al arm at δ_P = -1.10 ppm, a slight shift from 1.12 ppm is consistent with a change in aluminum coordination environment to give **3-pyr** (**Scheme 2**). Broadness of this ^{31}P NMR spectroscopic signal (despite the addition of excess heterocycle) and the persistence of diastereotopic CH_2 groups by ^1H NMR spectroscopy, supports a maintained P—Al interaction in **3-pyr**. Notably, dissolution of **3** in the weaker donor solvent, THF results in similarly shifted ^{31}P NMR resonances (δ_P = 36.6 and -3.4 ppm), suggestive of adduct formation to give **3-THF**. For THF, this reaction was found to be reversible on exposure to vacuum, returning complex **3**; this is not the case for pyridine as **3-pyr** persists despite the introduction of vacuum. Extended exposure of **3** to excess pyridine leads to decomposition, affording aluminum-free products (a diphosphine ligand containing a benzyl pendent group) *via* cleavage of the Al–C bond.

Adduct formation to give **3-pyr** and **3-THF** is thermodynamically downhill (ΔG° = –26.4 kcal·mol^{-1} for pyridine (**3-pyr**) and ΔG° = –22.4 kcal·mol^{-1} for THF (**3-THF**)). The optimized structure of both depicts a distorted trigonal bipyramidal alumatrane[35–37] where three X-type ligands are arranged equatorially, with two dative donors occupying both axial coordination sites. Upon adduct formation, the P—Al bond length elongates from 2.432 Å to 2.621 and 2.593 Å, for **3-pyr** and **3-THF**, respectively. This outcome supports our hypothesis: addition of an L-type donor to **3** weakens the P—Al interaction.

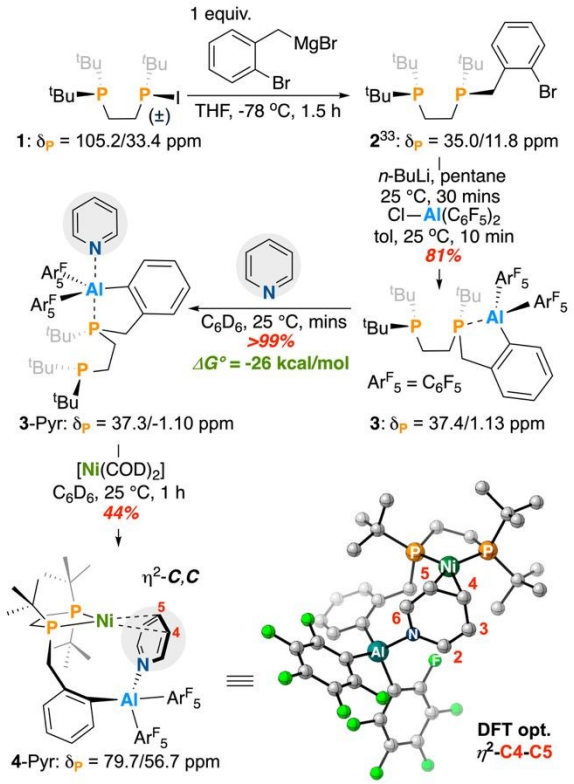

Scheme 2. Synthetic pathway towards aluminum-functionalized diphosphine **2** and its coordination to nickel(0). ΔG° value calculated using DLPNO-CCSD(T) (see ESI).

We next studied metalation. As implied by the stability of **3**, its combination with $[Ni(COD)_2]$ (COD = 1,5-cyclooctadiene) in C_6D_6 resulted in null reactivity. Given the propensity of **3** to coordinate weak donors such as THF, however, we wondered whether ring-opening could be donor-induced. In accord, the abovementioned reaction was repeated in the presence of 1 equiv. of pyridine, giving **3-pyr** *in-situ*. Addition of $[Ni(COD)]_2$ to this mixture generated two signals at δ_P = 79.7 and 56.7 ppm ($J_{P,P}$ = 58.5 Hz) by $^{31}P\{^1H\}$ NMR spectroscopy. Pyridine coordination and COD dissocation at nickel was confirmed by LIFDI-MS where a $[M]^+$ signal was observed at *m/z* = 849.179 (calcd. = 849.180 for $C_{38}H_{42}NAlF_{10}NiP_2^+$) of the appropriate isotope pattern. This compound was assigned as **4-pyr**, whose chemical shifts are close to a related η^2-bonded aryl Ni diphosphine complex synthesized by Fryzuk, which features ^{31}P peaks at δ_P = 79.5 and 40.2 ppm ($J_{P,P}$ = 102.9 Hz).[33] Of note, **4-pyr** can exist as one of six possible isomers: two of which are η^2-*N,C* and four of which are η^2-*C,C* bound. These isomeric possibilities are discussed in detail below.

Upon work-up, the ^1H NMR spectrum of **4-pyr** displayed

View Article Online
DOI: 10.1039/D6CC01343K

broadened peaks at δ_H = 4.21 and 3.71 ppm, both *significantly* upfield of typical pyridine ^{1}H environments (δ_H = 6.66-8.53 ppm in C_6D_6).[38] Three additional resonances (five total) include a multiplet at δ_H = 5.26 and broadened downfield-shifted signals at 6.40 and 8.43 ppm, which exhibit clear coupling by ^{1}H–^{1}H COSY NMR spectroscopy. These shifts, assigned to a major pyridine-bound isomer, are partnered with a second, minor secondary component having similar chemical shifts, suggesting the presence of isomers (*vide supra*) – this is shown in the 1D TOCSY NMR spectrum depicted in **Scheme 3a**. Proving these five signals are pyridine derived, use of pyridine-d_5 gives **4-pyr-d$_5$**, having the same ^{31}P signatures though the five pyridine ^{1}H NMR signals described previously are expectedly absent.

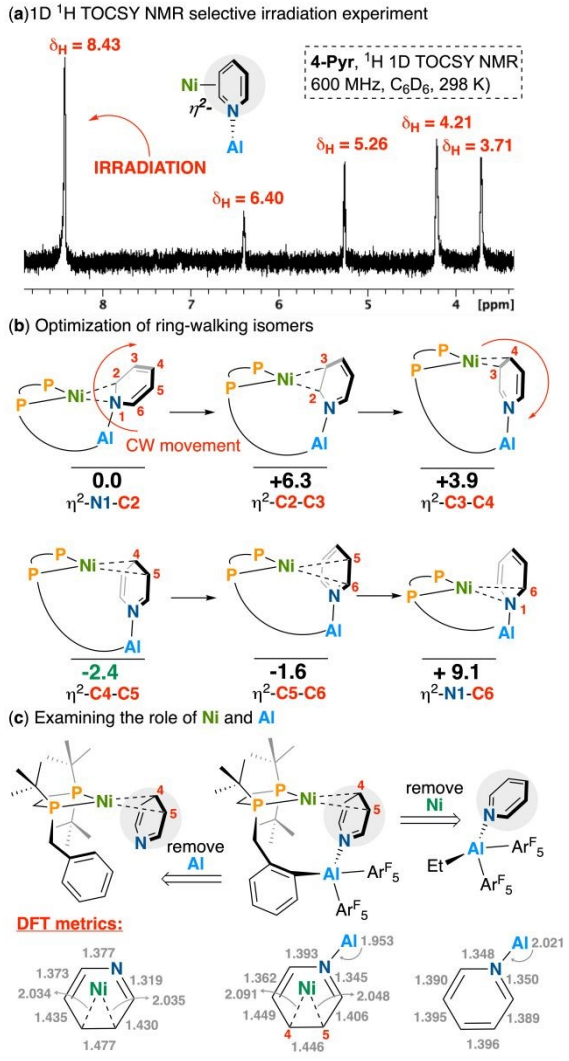

Scheme 3. (a)1D ^{1}H TOCSY selective irradiation experiment; (b) Optimization of pyridine ring-walking isomers; (c) Examining the role of Ni and Al. ΔG° values in kcal/mol, calculated using DLPNO-CCSD(T) (see ESI).

Altogether, these features are consistent with a high degree of nickel (dπ)-to-pyridine (CC)π* back-donation, an interaction that is mediated by aluminum. This supposition is further buttressed by a lack of observed exchange between **4-pyr-d$_5$** and free pyridine. It is worth underscoring that despite the ubiquity of heterocycle upgrading reactions using nickel and their linked intermediacy in pyridine functionalization reactions – examples of late metal η^2-pyridine complexes such as these are exceptionally rare.

Despite our best efforts, X-ray quality crystals of **4-pyr** could not be obtained, prompting the use of computational chemistry to assess structural possibilities. Although this rules out an unambiguous assignment, our NMR spectroscopic (symmetry/chemical shifts) and computational data (energies) suggest the η^2-C4-C5 and η^2-C3-C4 geometries to be most likely (**Scheme 3b**). Indeed, given the inherent asymmetry found in the Ni(diphosphine) framework, six pyridine-bound isomers are all possible, each of which reveals significant disruption of pyridine aromaticity. By arbitrarily assigning the η^2-N1-C2 geometry as having an energy of 0 kcal/mol, movement in a clockwise geometry cycles through 5/6 possible isomers with the η^2-C4-C5 isomer being the global minimum.[39–41] For the η^2-C4-C5 isomer, the Ni-bound C–C bond is elongated to 1.446 Å (**Scheme 3b**). In contrast, optimized structures of both free pyridine and its adduct with Al(C_6F_5)$_2$Et display uniform bond lengths consistent with aromatic character (pyridine: C–N = 1.342 Å, C–C = 1.398, 1.395 Å; pyridine–Al(C_6F_5)$_2$Et: C–N = 1.35 Å, C–C = 1.39, 1.40 Å). To evaluate the individual contributions of Ni and Al to substrate activation, we also optimized a structure in which pyridine is η^2-C4-C5-bound to Ni in the absence of Al. While this species also shows dearomatization, its C–N bonds are shorter (1.377, 1.319 Å) compared to those in η^2-C4-C5 **4-pyr** (1.393, 1.345 Å), suggesting a cooperative activation effect from both metal centers.

Expanding scope to a less symmetric heterocycle, we next assessed the reactivity of **3** with quinoline. Unlike pyridine, quinoline could give a series of two isomers that differ in the position of the quinoline *N*-heterocycle (whether it is *syn*- or *anti*-) in relation to the P-Al-containing arm (**Scheme 4**). By arbitrarily assigning the *syn*-η^2-N1-C2 geometry as having an energy of 0 kcal/mol, clockwise movement from *syn*-η^2-N1-C2 through to *syn*-η^2-C4-C5 shows *syn*-η^2-N1-C2 to be a minimum, whereas the *syn*-η^2-C4-C5 isomer was the global maximum (+10 kcal/mol); η^2-C5-C6 and η^2-C6-N1 isomers were not modelled for either *syn*- or *anti*- as these include an interaction between Ni and a ring junction carbon (which would, in principle, dearomatize the adjoining benzene ring, incurring an energetic penalty), as was observed from the η^2-C4-C5 isomer.

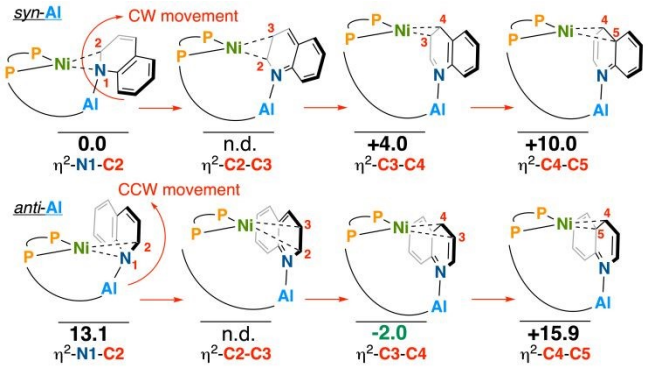

Scheme 4. Optimization of quinoline ring-walking isomers. ΔG° values in kcal/mol, calculated using DLPNO-CCSD(T) (see ESI). n.d. = not determined/located.

The *syn*-η^2-C2-C3 was not located as it converges to the more stable *syn*-η^2-C1-C2 isomer. Efforts to obtain a structure for the *anti*-η^2-C2-C3 isomer (**Scheme 4**) resulted in the most stable *anti*-η^2-C3-C4 isomer (-2.0 kcal/mol), though the *syn*-η^2-N1-C2 and *syn*-η^2-C4-C5

View Article Online
DOI: 10.1039/D6CC01343K

were calculated to be high in energy (+13.1 and +15.9 kcal/mol, respectively). Repeated convergence to the *anti*-η^2-C3-C4 isomer structure suggests this coordination mode is a dominant minimum on the potential energy surface.[42]

In practice, reaction of **3**, $[Ni(COD)_2]$, and quinoline resulted in an instant color change from yellow to red. By $^{31}P\{^1H\}$ NMR spectroscopy, two major doublets at δ_P = 78.0 and 55.0 ppm ($J_{P,P}$ = 44.0 Hz) were revealed, assigned as an isomer of **5-quin**; a minor product was also observed at δ_P = 86.3 and 60.9 ppm ($J_{P,P}$ = 39.0 Hz) (**Scheme 5**). Atmospheric pressure chemical ionization mass spectrometry (LIFDI-MS) confirmed quinoline inclusion, giving an $[M]^+$ signal at *m/z* = 899.195 (calcd. = 899.195 for $C_{42}H_{44}AlF_{10}NNiP_2$). Further support for the structure of **5-quin** is provided from ^1H NMR spectroscopy, which displays two broadened upfield-shifted signals corresponding to activated quinoline at δ_H = 4.73 and 3.86 ppm. These resonances exhibit clear through-bond coupling by ^1H–^1H COSY NMR spectroscopy and show ^{31}P coupling to the P(*t*Bu)(BnAl) arm by ^1H–^{31}P HMBC NMR spectroscopy. Given the similarity of the ^1H chemical shifts in the two isomers, including δ_H = 4.90 and 3.92 ppm for the minor, this isomer likely arises by the benzenoid ring orienting on either side of the molecule.

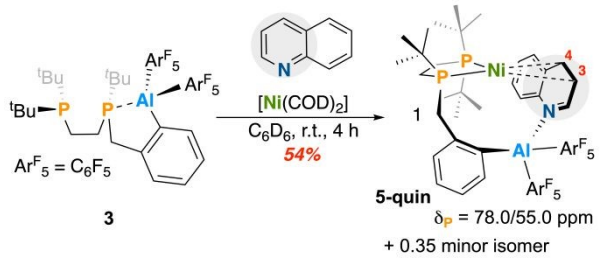

Scheme 5. Reaction of **3** with quinoline and $Ni(COD)_2$.

In conclusion, a new ambiphilic diphosphine ligand having a dative P—Al interaction has been prepared via lithium–halogen exchange and metalation using Cl—Al(C_6F_5)$_2$. Although this interaction is strong, addition of exogenous *N*-heterocycle weakens the Al-centered Lewis adduct, allowing for metalation using Ni(0). The resulting complexes feature η^2-coordination of the *N*-heterocycle to nickel. Both computational and spectroscopic data indicate significant substrate dearomatization, driven by nitrogen coordination to aluminum and back-donation from Ni into the pyridine π-system. These findings represent a new strategy for the cooperative binding and activation of synthetically and industrially relevant *N*-heterocycles. Ongoing efforts are focused on upgrading and transforming these cooperatively-bound substrates.

The authors are grateful to Western University, the Council of Ontario Universities for a John C. Polanyi award to M.W.D., the Canadian Foundation for Innovation (LOF-212442), and the Natural Sciences and Engineering Research Council of Canada (Discovery Grant, RGPIN-2020-04480 (M.W.D.), Discovery Launch Supplement, DGECR-2020-00183), and graduate award (CGRS-D to G.J.) for funding.

Data availability

The data supporting this article have been included as part of the Supplementary Information.

Conflicts of interest

There are no conflicts to declare.

References

1 V. T. Nguyen, R. N. Sladek, Y. Cao, N. Bhuvanesh, J. Zhou and O. V. Ozerov, *J. Am. Chem. Soc.*, 2024, **146**, 31281–31294.
2 C. M. Marshall, J. G. Federice, C. N. Bell, P. B. Cox and J. T. Njardarson, *J. Med. Chem.*, 2024, **67**, 11622–11655.
3 H. Cao, Q. Cheng and A. Studer, *Angew. Chem. Int. Ed.*, 2023, **62**, e202302941.
4 S. Maity, A. Bera, A. Bhattacharjya and P. Maity, *Org. Biomol. Chem.*, 2023, **21**, 5671–5690.
5 S. M. Khake and N. Chatani, *Chem*, 2020, **6**, 1056–1081.
6 A. D. Dilinaer, G. J. Jobin and M. W. Drover, *Dalton Trans.*, 2024, **53**, 13298–13307.
7 T. Zhang, Y.-X. Luan, N. Y. S. Lam, J.-F. Li, Y. Li, M. Ye and J.-Q. Yu, *Nat. Chem.*, 2021, **13**, 1207–1213.
8 J.-F. Li, D. Pan, H.-R. Wang, T. Zhang, Y. Li, G. Huang and M. Ye, *J. Am. Chem. Soc.*, 2022, **144**, 18810–18816.
9 Y.-X. Luan and M. Ye, *Chem. Commun.*, 2022, **58**, 12260–12273.
10 Y. Nakao, K. S. Kanyiva and T. Hiyama, *J. Am. Chem. Soc.*, 2008, **130**, 2448–2449.
11 M. M. Shoshani, *Cell Rep. Phys. Sci.*, 2023, **4**, 101213.
12 V. Singh, Y. Nakao, S. Sakaki and M. M. Deshmukh, *J. Org. Chem.*, 2017, **82**, 289–301.
13 C.-C. Tsai, W.-C. Shih, C.-H. Fang, C.-Y. Li, T.-G. Ong and G. P. A. Yap, *J. Am. Chem. Soc.*, 2010, **132**, 11887–11889.
14 N. Hara, N. Uemura and Y. Nakao, *Chem. Commun.*, 2021, **57**, 5957–5960.
15 Y. Kuroda, K. Park, Y. Shimazaki, R.-L. Zhong, S. Sakaki and Y. Nakao, *Angew. Chem. Int. Ed.*, 2023, **62**, e202300704.
16 H. Gao, L. Hu, Y. Hu, X. Lv, Y.-B. Wu and G. Lu, *Catal. Sci. Technol.*, 2021, **11**, 4417–4428.
17 B. Jiang, J.-M. Liu and S.-L. Shi, *ACS Catal.*, 2023, **13**, 6068–6075.
18 J.-F. Li, W.-W. Xu, R.-H. Wang, Y. Li, G. Yin and M. Ye, *Nat. Commun.*, 2021, **12**, 3070.
19 J.-B. Ma, X. Zhao, D. Zhang and S.-L. Shi, *J. Am. Chem. Soc.*, 2022, **144**, 13643–13651.
20 W.-C. Shih and O. V. Ozerov, *J. Am. Chem. Soc.*, 2017, **139**, 17297–17300.
21 W.-C. Shih, W.-C. Chen, Y.-C. Lai, M.-S. Yu, J.-J. Ho, G. P. A. Yap and T.-G. Ong, *Org. Lett.*, 2012, **14**, 2046–2049.
22 R. P. Singh, S. Sinhababu and N. P. Mankad, *ACS Catal.*, 2023, **13**, 12519–12542.
23 Y.-X. Wang, S.-L. Qi, Y.-X. Luan, X.-W. Han, S. Wang, H. Chen and M. Ye, *J. Am. Chem. Soc.*, 2018, **140**, 5360–5364.
24 J. Zhou and B.-F. Shi, in *Transition-Metal-Catalyzed C-H Functionalization of Heterocycles*, 2023, pp. 357–392.
25 Y. Nakao, Y. Yamada, N. Kashihara and T. Hiyama, *J. Am. Chem. Soc.*, 2010, **132**, 13666–13668.
26 J. Becica and G. E. Dobereiner, *Org. Biomol. Chem.*, 2019, **17**, 2055–2069.
27 A. Bhunia, K. Bergander and A. Studer, *J. Am. Chem. Soc.*, 2018, **140**, 16353–16359.
28 G. Bouhadir and D. Bourissou, *Chem. Soc. Rev.*, 2016, **45**, 1065–1079.
29 Y. Zhang, Q. Ni, L. Jiang, R. Cao and L. Qiu, *Eur. J. Org. Chem.*, 2025, **28**, e202401100.
30 G. Song, B. Wang, M. Nishiura and Z. Hou, *Chem. -Eur. J.*, 2015, **21**, 8394–8398.
31 Q. Sun, P. Chen, Y. Wang, Y. Luo, D. Yuan and Y. Yao, *Inorg. Chem.*, 2018, **57**, 11788–11800.
32 A. C. Zimmerman and M. D. Fryzuk, *Organometallics*, 2019, **38**, 3671–3679.

View Article Online
DOI: 10.1039/D6CC01343K

33 A. C. Zimmerman and M. D. Fryzuk, *Organometallics*, 2018, **37**, 2305–2318.
34 N. A. Shcherbina, I. V. Kazakov, A. V. Pomogaeva, A. S. Lisovenko, M. A. Kryukova, D. A. Doinikov, N. Yu. Gugin, Y. V. Kondrat'ev and A. Y. Timoshkin, *J. Organomet. Chem.*, 2021, **948**, 121909.
35 A. K. Phukan and A. K. Guha, *Inorg. Chem.*, 2011, **50**, 1361–1367.
36 W. Su, Y. Kim, A. Ellern, I. A. Guzei and J. G. Verkade, *J. Am. Chem. Soc.*, 2006, **128**, 13727–13735.
37 W. Su, J. Kobayashi, A. Ellern, T. Kawashima and J. G. Verkade, *Inorg. Chem.*, 2007, **46**, 7953–7959.
38 Z. Wang, X. Li, H. Sun, O. Fuhr and D. Fenske, *Organometallics*, 2018, **37**, 539–544.
39 A. Nova, M. Reinhold, R. N. Perutz, S. A. Macgregor and J. E. McGrady, *Organometallics*, 2010, **29**, 1824–1831.
40 S. A. Johnson, N. M. Mroz, R. Valdizon and S. Murray, *Organometallics*, 2011, **30**, 441–457.
41 T. A. Ateşin, T. Li, S. Lachaize, J. J. García and W. D. Jones, *Organometallics*, 2008, **27**, 3811–3817.
42 J. J. Garcia, N. M. Brunkan and W. D. Jones, *J. Am. Chem. Soc.*, 2002, **124**, 9547–9555.

View Article Online
DOI: 10.1039/D6CC01343K

- The data supporting this article have been included as part of the Supplementary Information.